On numerical construction of worse-case convergence rates for Discrete-time Lurye systems with odd nonlinearities

Xinyi Wang, Jingfan Zhang, Joaquin Carrasco, and Peter Seiler

***Abstract*— This paper considers the asymptotic convergence rate of Lurye systems consisting of a discrete-time, LTI system in feedback with a nonlinearity. This work is motivated by convergence rate analysis of first-order optimization algorithms. Lurye analysis has been used in the literature to provide an upper bound on the worst-case convergence rate. If the nonlinearity is smooth then the asymptotic convergence rate is governed by the linearization near the equilibrium point. In this paper, we present a novel construction of nonlinearities that obtain slower convergence rates than the worst-case over smooth functions. In particular, our constructed nonlinearities are odd and have a fractal construction.**

I. INTRODUCTION

A Lurye system can be described as a negative feedback interconnection of a stable LTI plant G and a static slope-restricted nonlinearity ϕ whose slope is bounded in the range $[0,K]$, denoted as $\phi \in S[0,K]$, i.e.

$$0 \leq \frac{\phi(y_2)-\phi(y_1)}{y_2-y_1} \leq K, \tag{1}$$

for all $y_1, y_2 \in \mathbb{R}$ and $\phi(0)=0$. In this paper we focus our attention on odd nonlinearities, i.e. $\phi(y) = -\phi(-y)$. Furthermore, as the paper deals with convergence analysis, the autonomous Lurye system as in Figure 1 is considered.

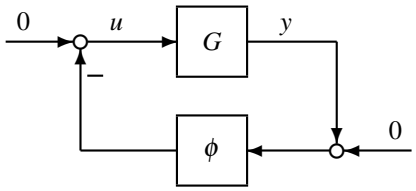

Fig. 1. Autonomous Lurye system

The Kalman conjecture [1] is a cornerstone to understand the development in absolute stability of Lurye systems. It states that the Lurye system is stable with all $\phi \in S[0,K]$ if and only if all linearized systems with ϕ replaced by a gain from 0 to K are stable. The Kalman conjecture in discrete-time is true for first order systems, but false for second order systems [2], [3].

In recent years, first order optimisation algorithms for strongly convex functions have been rewritten as Lurye systems, and the convergence rate of optimisation algorithms can be expressed as the exponential decay rate of the corresponding Lurye system [4]. Other relevant work on optimization analysis includes [5], [6], [7].

Let K_{AS} be the minimum gain for which the system is not absolutely stable. To date, the less conservative estimation of K_{AS} by the use of discrete-time Zames–Falb multipliers [8], [9]. The current result for searches on Zames–Falb multipliers [10] have been shown to be a very precise lower bound for absolute stability as it has been shown in [11].

If we restrict our analysis to nonlinearities $\phi \in S[0,K]$ with $K < K_{AS}$, all trajectories will converge to the origin, i.e. the nonlinear system is Globally Asymptotically Stable (GAS). One may think of the Kalman conjecture for convergence analysis as the following statement: the worst-case convergence rate of the class of asymptotically stable Lurye systems with G and $\phi \in S[0,K]$ is equal to the worst convergence rate of all its possible linearisations, i.e. replacing ϕ for any linear gain within $[0,K]$. If we restrict our attention to smooth nonlinearities, then the Kalman conjecture for convergence is valid as the nonlinear system will converge to the linearised system.

Nonetheless, it is not possible to linearise the system for non-smooth nonlinearities around the origin satisfying Equation 1. The Kalman conjecture for convergence analysis has been proved false when the nonlinearity ϕ is asymmetric to the origin [12]. To the best of authors' knowledge, the counterexample when the nonlinearity is odd does not exist in literature. Some previous examples in the literature about the convergence analysis [4], [13] show Lurye systems with periodic solutions, which is not asymptotically stable, so they cannot be considered as counterexamples to the Kalman conjecture for convergence.

In this manuscript, we provide the first numerical counterexample to the Kalman conjecture for convergence analysis when the nonlinearity is odd. This counterexample motivates the technique (eg. [4], [12], [14], [15], [16]) to bound the worst-case convergence rate of first order optimisation with convex functions. In addition, it is interesting to understand the conservativeness of the analysis by constructing nonlinearities leading to the worse convergence rates than the linear case.

II. KALMAN CONJECTURE FOR CONVERGENCE ANALYSIS

Consider the discrete-time nonlinear dynamical system S defined by

$$x_{k+1} = f(x(k)), \tag{2}$$

Department of Electrical & Electronic Engineering, School of Engineering, University of Manchester, M13 9PL, UK.
xinyiwang147@gmail.com
jingfan.zhang@manchester.ac.uk
joaquin.carrasco@manchester.ac.uk
P. Seiler is with the Department of Electrical Engineering & Computer Science, University of Michigan, Ann Arbor, US. pseiler@umich.edu
This work was supported in part by EPSRC project EP/S03286X/1.

where $x_k \in \mathbb{R}^n$ and $f : \mathbb{R}^n \to \mathbb{R}^n$. S is globally exponentially stable if there exist $\rho \in (0,1)$ and $c > 1$ such that

$$\|x_k\| \leq c\rho^k \|x_0\| \quad \forall k \geq 0,\ \forall x_0 \in \mathbb{R}^n. \tag{3}$$

If the system S is globally exponential stable, we define its converge rate as

$$\rho_S = \inf_{\rho} \{\rho \in (0,1) : \exists c > 1 \text{ such that } \|x_k\| \leq c\rho^k \|x_0\| \quad \forall k \geq 0,\ \forall x_0 \in \mathbb{R}^n\}. \tag{4}$$

Let $[A,B,C,0]$ be a minimal realisation of the LTI SISO strictly-proper system G, then the state-space description of the feedback system in Fig. 1 is given by

$$x_k = Ax_k - B\phi(Cx_k). \tag{5}$$

Henceforth, the convergence rate of absolute stable Lurye system between a plant G and a nonlinearity ϕ, in short $\{G,\phi\}$, is given by the denoted as $\rho_{\{G,\phi\}}$, and the worst-case convergence rate of the class of Lurye systems is defined as

$$\rho^*_{\{G,K\}} = \sup_{\phi \in S[0,K]} \{\rho_{\{G,\phi\}}\}, \tag{6}$$

A lower bound of $\rho^*_{\{G,K\}}$ is given by the linear case as

$$\underline{\rho^*_{\{G,K\}}} = \max_{\tau \in [0,1]} \left\{ |\bar{\lambda}(A - \tau KBC)| \right\}. \tag{7}$$

where $\bar{\lambda}(X)$ denotes the eigenvalue of the matrix X with the largest absolute value.

Finally, we translate the Kalman conjecture for the convergence analysis as follows.

Conjecture 1: For any $G \in \mathbf{RH}_\infty$, let $\phi \in S[0,K]$ such that the feedback interconnection between G and any ϕ is stable, then

$$\rho^*_{\{G,K\}} = \underline{\rho^*_{\{G,K\}}}. \tag{8}$$

This paper focuses on odd-nonlinearities. As in the non-odd case [12], the nonlinearity is required to be non-differentiable at the origin. However, the odd condition requires a more sophisticated nonlinearity than a simple change of slope at the origin.

We say the the Lurye system in Figure 1 has a ρ-periodic orbit with period T if $y(k) = \rho^T y(k-T)$. In this case, the output of LTI system decays to zero with exponential converge rate ρ.

III. Numerical counterexamples

In this section, we present some numerical counterexamples to Conjecture 1. Namely, we show that $\rho^*_{\{G,K\}} > \underline{\rho^*_{\{G,K\}}}$ is possible, so it is not tight to bound the worst-case convergence rate of a Lurye system by its linearisation.

Let us consider the plant G

$$G(z) = \frac{0.1z}{z^2 - 1.8z + 0.81}, \tag{9}$$

with a state-space representation given by

$$A = \begin{bmatrix} 0 & 1 \\ -0.81 & 1.8 \end{bmatrix}, \quad B = \begin{bmatrix} 0 \\ 1 \end{bmatrix}, \quad C = \begin{bmatrix} 0 & 0.1 \end{bmatrix}. \quad D = 0.$$

We denote the initial condition $x(0) = \begin{bmatrix} x_1(0) & x_2(0) \end{bmatrix}^\top$.

In the rest of the section, we explore different nonlinearities that produce worse convergence rates than the worst linear convergence rate. All nonlinearities belongs to the sector $[0,13]$, hence $\underline{\rho^*_{\{G,K\}}} = 0.9$.

The class of nonlinearities to achieve worse convergence rates is parametrised as follows. If $y > 0$, then

$$\phi_{\kappa,\eta}(y) = \begin{cases} c_1 \kappa^N & \text{if } \kappa^N \leq y < \eta\kappa^N, \\ 13y + c_2 \kappa^N & \text{if } \eta\kappa^N \leq y < \kappa^{N+1}; \end{cases} \tag{10}$$

where N is the maximum integer that is smaller than $\log_\kappa(y)$, $\kappa > 1$ and $1 < \eta < \kappa$. If $y < 0$, then $\phi_{\kappa,\eta}(y) = -\phi_{\kappa,\eta}(-y)$. Moreover, $\phi_{\kappa,\eta}(0) = 0$. To achieve continuity in the changes of slope, the parameters c_1 and c_2 must be selected such that

$$c_1 = 13\eta + c_2; \tag{11}$$

$$\kappa c_1 = 13\kappa + c_2, \tag{12}$$

i.e.

$$c_1 = 13\frac{\kappa - \eta}{\kappa - 1}; \tag{13}$$

$$c_2 = 13\left(\frac{\kappa - \eta}{\kappa - 1} - \kappa\right). \tag{14}$$

This fractal construction of the nonlinearity is key to achieve an asymptotic behavior slower than the linear case.

By construction, the nonlinearity is continuous in the interval $(0,\infty)$ and is differentiable almost everywhere, hence

$$0 \leq \frac{\phi_{\kappa,\eta}(y_2) - \phi_{\kappa,\eta}(y_1)}{y_2 - y_1} \leq 13,$$

for all $y_1, y_2 > 0$. This nonlinearity can be seen the gradient of a convex function [17], so it can be used in the context of optimization algorithms [4] as the counterexample in [12].

The simulations will generate a sequence of pairs $\{(y_k, \phi_{\kappa,\nu}(y_k))\}_{k=1}^{N_{\text{steps}}}$. As these sequences converge to zero, it is helpful to plot the sequences $\{(y_k\kappa^{-N}, \phi_{\kappa,\nu}(y_k\kappa^{-N}))\}_{k=1}^{N_{\text{steps}}}$, where N is defined as in Equation 10. By definition $y_k\kappa^{-N} \in [1,\kappa)$. Henceforth, the map defined by the sequence of pairs $\{(y_k\kappa^{-N}, \phi_{\kappa,\nu}(y_k\kappa^{-N}))\}_{k=1}^{N_{\text{steps}}}$ is referred to as the projected nonlinearity.

A. Example 1

As first example, we fix $\kappa = 10$ and we produce a linear search over the parameter η, obtaining worse convergence rates than the worst linear convergence rate for $\eta = 9/5$. The fractal behaviour of the nonlinearity is depicted in Figures 2.

The convergence rate of the Lurye system with G and $\phi_{10,\frac{9}{5}}$ is shown in Fig. 3. The real convergence rate is about 0.924 hence it is above the worse linear convergence rate for the system, i.e. 0.9. As a result, the system exhibits trajectories which are slower than the linearised trajectory.

If we increase the number of steps, it is interesting to see how the dynamics escapes to a faster dynamics for a significant number of steps, recovering the slower dynamics later, see Figure 4.

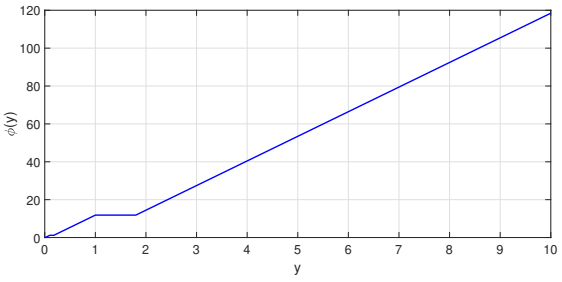

Fig. 2. $\phi_{10,\frac{9}{5}}(y)$ when $0 < y \leq 10$

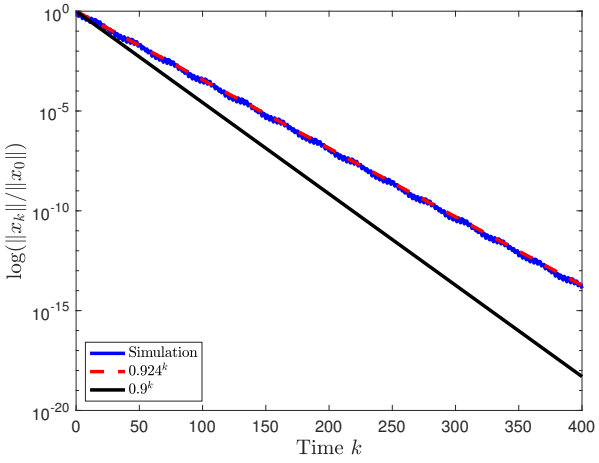

Fig. 3. Similation of the Lurye system between G and $\phi_{10,\frac{9}{5}}$ with $x(0) = [-0.6775, -0.2896]^\top$.

Although the nonlinearity $\phi_{10,\frac{9}{5}}$ has shown the required structure to excite slower dynamics, its convergence rate is not constant. To show this, we project the nonlinearity into the interval $[1,10]$, i.e. instead of plotting the pairs $\{(y_k, \phi_{10,\frac{9}{5}}(y_k))\}_{k=1}^{N_{\text{steps}}}$, we plot the pairs $\{(y_k 10^{-N}, \phi_{10,\frac{9}{5}}(y_k 10^{-N}))\}_{k=1}^{N_{\text{steps}}}$, where N has been defined below Equation 10. Figures 5 and 6 clearly demonstrate that the system is not able to keep a stable ρ-periodic behaviour, the simulation uses a limited range of the project nonlinearity initially but it is not preserved when the number of steps increases to 4000.

We can demonstrate the lack of stable periodic orbits by plotting an estimation of the asymptotic convergence rate. We run experiments of 6000 steps and compute the average decay for the last 2000 steps with 25×10^4 equidistant initial conditions in the square $[-1,1] \times [-1,1]$. There are small regions in Fig. 7 with an homogenous colour, denoting the existence of a quasi-stable ρ-periodic orbit with $\rho \sim 0.9153$ and period $T = 26$, as stable ρ-periodic orbits require the condition $\kappa = \rho^{-T}$, however $0.9153^{-26} = 9.985 \neq 10$.

B. Example 2

The second example is obtained using a Monte-Carlo search over the free parameters κ and η, a stable convergence

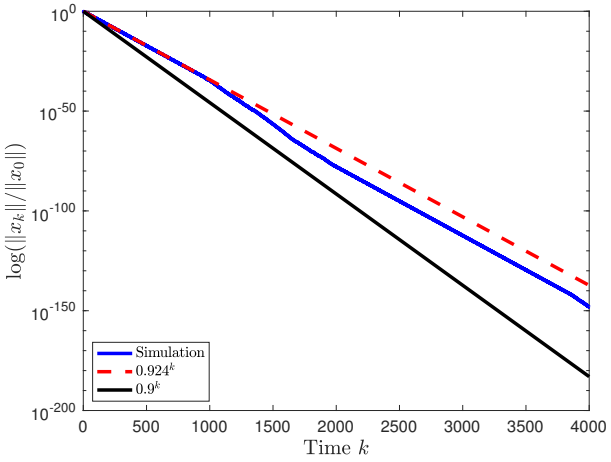

Fig. 4. When the same simulation as in Figure 3 is run for 4000 steps, the generated behaviour is not stable and the simulation switches between difference local convergences rates.

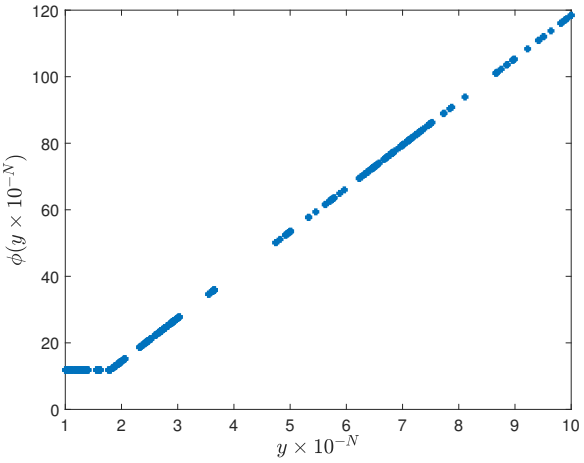

Fig. 5. For the first 400 steps, the simulation uses a reduced range of the "projected" nonlinearity

rate of $\rho = 0.9293$ is achieved over 8000 steps when $\kappa = 5.8139$ and $\eta = 1.7294$.

As in the previous example, we can explore the stability of the orbit by projecting the nonlinearity into the interval $[1, \kappa]$, i.e. instead of plotting the pairs $\{(y_k, \phi_{5.8139,1.7294}(y_k))\}_{k=1}^{N_{\text{steps}}}$, we will plot the pairs $\{y_i \times \kappa^{-N}, \phi_{5.8139,1.7294}(y_i \times \kappa^{-N})\}_{k=1}^{N_{\text{steps}}}$, where N has been defined below Equation 10. After a short transient, only 24 points of the nonlinearity are used as shown in Figure 9. Besides numerical precision, the solution has a ρ-periodic orbit, i.e. $y(k) = \rho^{24} y(k-24)$. As mentioned, there is a relationship between the achieved convergence rate, the parameter κ and the period of the orbit, i.e.

$$\kappa = \rho^{-T} = \rho^{-24}. \tag{15}$$

It is worth highlighting that the slower convergence rate is achieved for 10^4 random initial conditions in the square $[-1,1] \times [-1,1]$. The orbit is achieved in all simulations, and

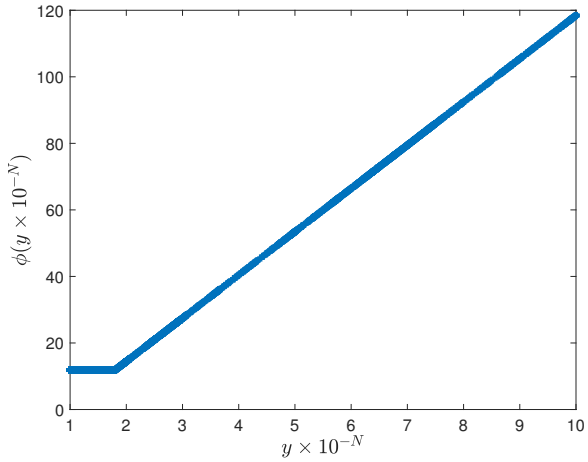

Fig. 6. For 4000 steps, the simulation uses the whole range of the "projected" nonlinearity

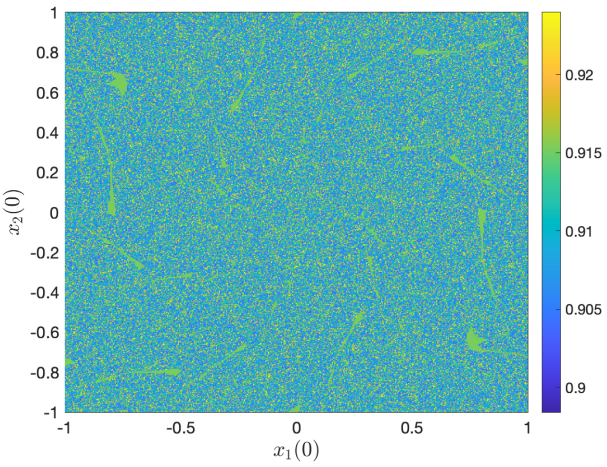

Fig. 7. Estimation of the asymptotic converge rate last 1000 steps for 6000-step simulations of the Lurye system with G and $\phi_{10,\frac{9}{5}}$ with 250,000 different initial conditions in the square $[-1,1]\times[-1,1]$.

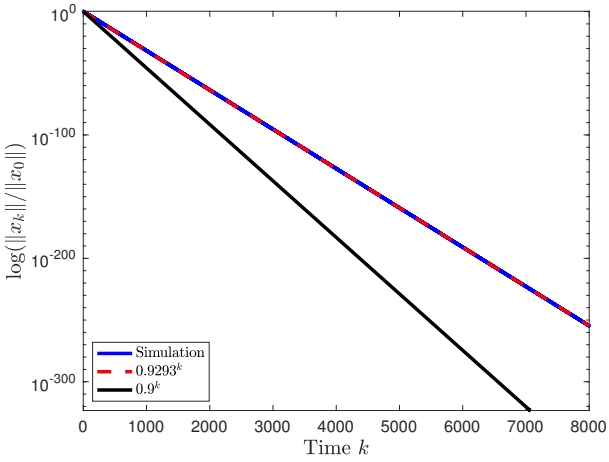

Fig. 8. Simulation of the Lurye system with G and $\phi_{5.8139,1.7294}$

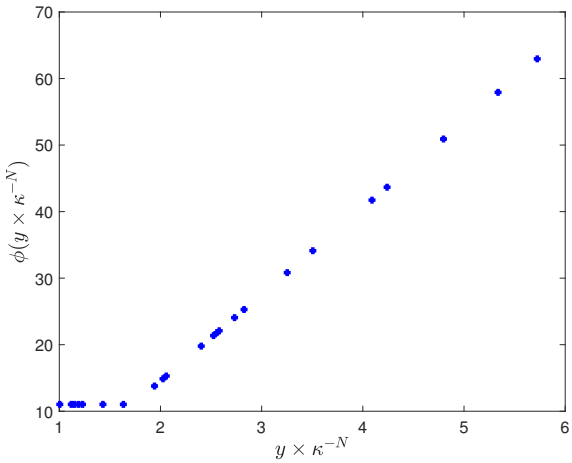

Fig. 9. "Projected" nonlinearity for the last 5000 step of the simulation in Figure 8.

if we take the last 24 samples, we obtain the average value of $\rho = 0.929281272622455$, with a standard deviation of 9.59×10^{-15} due to numerical precision, showing the stability of the ρ periodic orbit.

The orbit can be generated by the following initial condition

$$x(0) = \begin{bmatrix} 24.02986945329326 \\ 32.52678579052714 \end{bmatrix}.$$

With this initial condition, $|y(k) - \rho^{24} y(k-24)| < 10^{-14}$ for all $24 \leq k \leq 8000$. As this correspond with the machine numerical precision, we conclude that the orbit is stable. Once the convergent orbit has been found numerically, the analytical expression of the initial condition can be obtained with the same procedure as used in [12], as $x(0)$ is the eigenvector associated with the eigenvalue ρ^{-24} of the transition matrix T_{24}, where $x(24) = T_{24}x(0)$. Note that T_{24} is constructed by the a prior knowledge provided by the numerical orbit.

C. Example 3

The last example uses the same definition as in Equation 10, but with the parameters $\kappa = 5.6233$ and $\eta = 1.7177$. All initial conditions tested during the simulations lead to one of two different stable ρ-periodic behavior, one mode with $\rho_1 = \kappa^{-1/24} \simeq 0.9306$ and $\rho_2 = \kappa^{-1/21} \simeq 0.9210$.

By using 250,000 equidistant initial conditions in the square $[-1,1]\times[-1,1]$, the rate of convergence of the last 2000 steps for the obtained trajectory is shown in Figure 10. We can observe the bi-modal structure of the problem. Both modes of convergence are slower than the worst linear convergence rate.

As expected by the construction of the nonlinearity, the behaviour of the initial condition preserves the fractal pattern. So if the initial conditions are taken in the square $[-\kappa^{-1},\kappa^{-1}]\times[-\kappa^{-1},\kappa^{-1}]$, the same pattern is generated, see Figure 11.

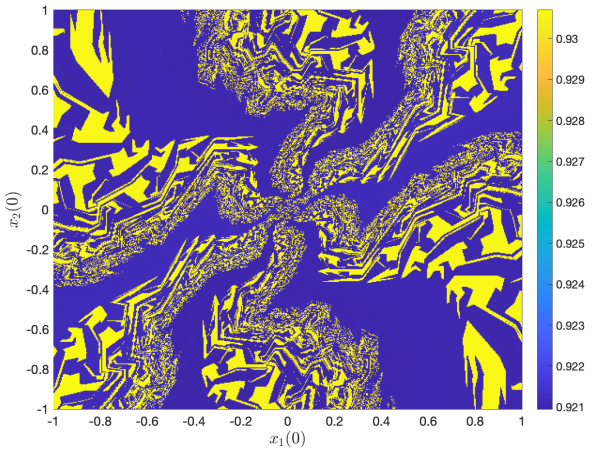

Fig. 10. Convergence rate of the last 200 periods for 8000-step simulations of the Lurye system with G and $\phi_{5.6233,1.7177}$ with 250,000 different initial conditions in the square $[-1,1]\times[-1,1]$.

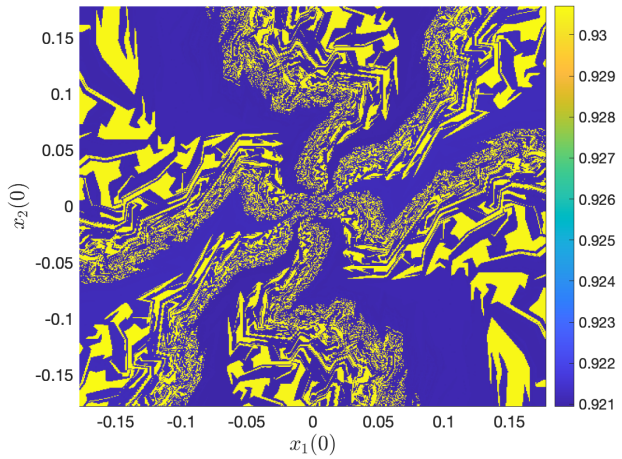

Fig. 11. Convergence rate of the last 200 periods for 8000-step simulations of the Lurye system with G and $\phi_{5.6233,1.7177}$ with 250,000 different initial conditions in the square $[-\kappa^{-1},\kappa^{-1}]\times[-\kappa^{-1},\kappa^{-1}]$.

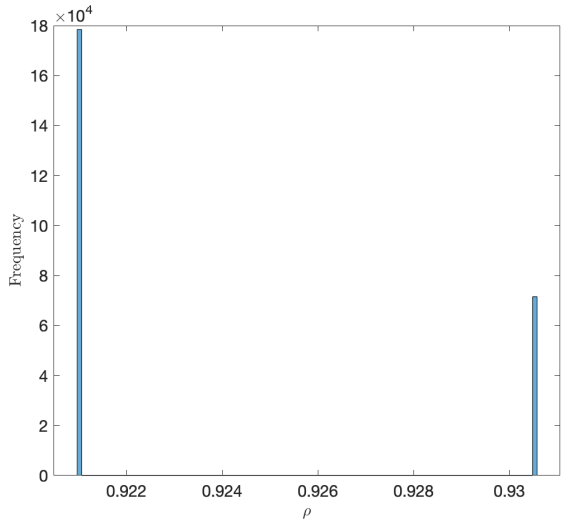

Fig. 12. Distribution of the achieved convergence rate of the Lurye system with G and $\phi_{5.6233,1.7177}$ over the last period of an 8000 step simulation with the 250,000 different initial conditions in Figure 10.

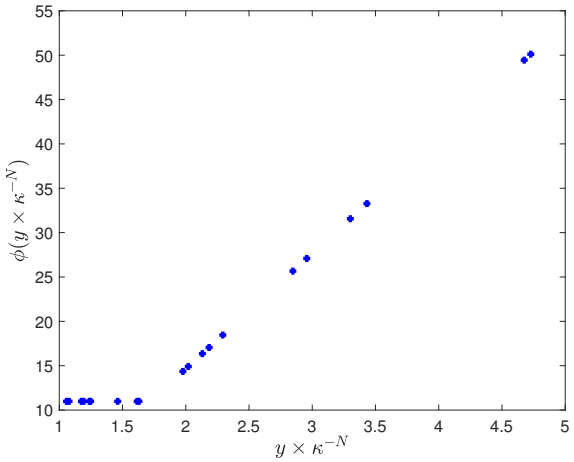

Fig. 13. "Projected" nonlinearity for the last 5000 step of the simulation in Figure 10 for the faster convergence rates ($\rho=\kappa^{-1/21}$).

The faster convergence rate is obtained for 71.26% of the initial conditions, where the slower converge rate is obtained for 28.74% of the initial conditions, see Figure 12. The simulations with the faster convergence rate achieve a ρ-periodic behaviour with period 21 (see Figure 13 for the shape of the period), whereas the simulations with slower convergence rate achieve a ρ-periodic behaviour with period 24 (see Figure 14 for the shape of the period). As expected from Equation 15, a longer period of the orbit implies a slower convergence rate for the same value of the parameter κ.

IV. Discussion

The analysis with Zames–Falb multiplier has been shown to have little conservativeness for the case $\rho=1$, where an automatic construction of the nonlinearity to achieve a periodic behaviour has been proposed in [11]. For the plant in our example, the analysis with Zames–Falb multipliers ensure the stability for the interval $K\in[0,1.3511322]$ and it is possible to construct a counterexample of the Kalman Conjecture for $K=1.3575410$, where this gain is analytically provided with the help of the phase Bode plot as shown in [18].

For the case $\rho<1$, the main challenge is the construction of a nonlinearity that generates nonlinear asymptotic convergence behavior. With this aim, we must use of type of nonlinearities that preserves the nonlinear behaviour at any neighbourhood of the origin. For the non-odd case, we can use a simple construction for nonlinearities as shown in [12], where the nonlinearity has two different constant slopes, one for positive inputs and a different one for negative inputs. An analytic construction of the convergence rate is achieved.

In this paper we show that this is also possible for

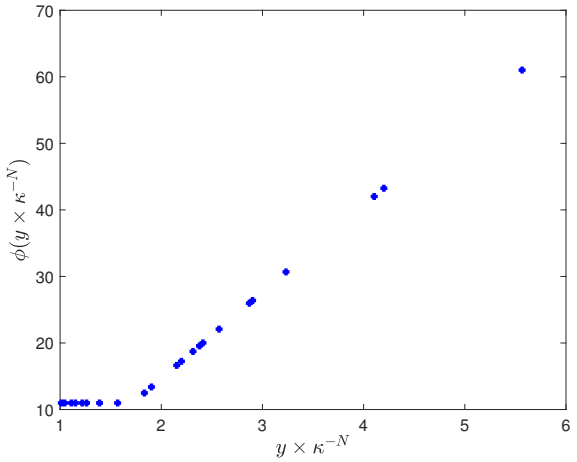

Fig. 14. "Projected" nonlinearity for the last 5000 step of the simulation in Figure 10 for the faster convergence rates ($\rho = \kappa^{-1/24}$).

odd nonlinearities, although a symbolic construction is very challenging. A fractal construction of the nonlinearity is required. Nonetheless, there is still a significant gap between the convergence generated by these examples, $\rho \sim 0.930$, and the upper bound provided by the Zames-Falb analysis in [12], $\bar{\rho} = 0.9965$.

In comparison with [11], the analytical construction becomes significantly more challenging as the monotonicity condition is not limited to a single period. On the other hand, we have shown that the initial conditions are not critical to detect if a nonlinearity provides worse-rates than the worst linear case, therefore numerical construction is less challenging than the case $\rho = 1$.

Finally, it is worth highlighting that we have used more complex nonlinearities. In the spirit of [11], we have searched nonlinearities with more complex structure, e.g.

$$\phi_2(y) = \begin{cases} c_1\kappa^N & \text{if } \kappa^N \leq y < \eta_1\kappa^N, \\ 13y + c_2\kappa^N & \text{if } \eta_1\kappa^N \leq y < \eta_2\kappa^N, \\ c_3\kappa^N & \text{if } \eta_2\kappa^N \leq y < \eta_3\kappa^N, \\ 13y + c_4\kappa^N & \text{if } \eta_3\kappa^N \leq y < \kappa^{N+1}; \end{cases} \tag{16}$$

where c_1, c_2, c_3, and c_4 are selected to ensure the continuity of the nonlinearity. However, no improvement has been found.

As future work, duality conditions for the modified class of Zames-Falb multipliers developed by [19] could be found. They may be useful to show the existence of a ρ-periodic behavior as in [18], [11].

V. Conclusion

In this manuscript, a counterexample to the Kalman conjecture for convergence analysis is constructed with an odd slope-restricted nonlinearity, i.e. we construct nonlinearities where the Lurye system converges to the origin with worse-convergence rates than This counterexample shows that the lower bound provided by the linear case is not tight for the corresponding Luyre systems. This result, together with the counterexample with non-odd nonlinearity [12], motivates the techniques to estimate an upper bound of the convergence rate.

As discussed above, it remains open the question about the conservativeness of the use of the subclass of Zames-Falb multipliers for the bound of convergence rates.

References

[1] R. E. Kalman, "Physical and mathematical mechanisms of instability in nonlinear automatic control systems," *Transactions of ASME*, vol. 79, pp. 553–566, 1957.

[2] J. Carrasco, W. P. Heath, and M. de la Sen, "Second-order counterexample to the discrete-time kalman conjecture," in *2015 European Control Conference (ECC)*, 2015, pp. 981–985.

[3] W. P. Heath, J. Carrasco, and M. de la Sen, "Second-order counterexamples to the discrete-time Kalman conjecture," *Automatica*, vol. 60, pp. 140 – 144, 2015.

[4] L. Lessard, B. Recht, and A. Packard, "Analysis and design of optimization algorithms via integral quadratic constraints," *SIAM Journal on Optimization*, vol. 26, no. 1, pp. 57–95, 2016.

[5] Y. Drori and M. Teboulle, "Performance of first-order methods for smooth convex minimization: a novel approach," *Mathematical Programming*, vol. 145, pp. 451–482, 2014.

[6] A. B. Taylor, J. M. Hendrickx, and F. Glineur, "Performance estimation toolbox (pesto): Automated worst-case analysis of first-order optimization methods," in *2017 IEEE 56th Annual Conference on Decision and Control (CDC)*, 2017, pp. 1278–1283.

[7] Y. Nesterov, *Introductory lectures on convex optimization: A basic course*. Springer Science & Business Media, 2013, vol. 87.

[8] R. O'Shea and M. Younis, "A frequency-time domain stability criterion for sampled-data systems," *IEEE Transactions on Automatic Control*, vol. 12, no. 6, pp. 719–724, December 1967.

[9] J. Willems and R. Brockett, "Some new rearrangement inequalities having application in stability analysis," *IEEE Transactions on Automatic Control*, vol. 13, no. 5, pp. 539–549, October 1968.

[10] J. Carrasco, W. P. Heath, J. Zhang, N. S. Ahmad, and S. Wang, "Convex searches for discrete-time Zames-Falb multipliers," *IEEE Transactions on Automatic Control*, vol. 65, no. 11, pp. 4538–4553, 2020.

[11] P. Seiler and J. Carrasco, "Construction of periodic counterexamples to the discrete-time Kalman conjecture," *IEEE Control Systems Letters*, vol. 5, no. 4, pp. 1291–1296, 2021.

[12] J. Zhang, P. Seiler, and J. Carrasco, "Zames-Falb multipliers for convergence rate: motivating example and convex searches," *International Journal of Control*, in press.

[13] B. V. Scoy, R. A. Freeman, and K. M. Lynch, "The fastest known globally convergent first-order method for minimizing strongly convex functions," *IEEE Control Systems Letters*, vol. 2, no. 1, pp. 49–54, 2018.

[14] R. Boczar, L. Lessard, A. Packard, and B. Recht, "Exponential stability analysis via integral quadratic constraints," *eprint arXiv: 1706.0133*, 2017.

[15] S. Michalowsky, C. Scherer, and C. Ebenbauer, "Robust and structure exploiting optimisation algorithms: an integral quadratic constraint approach," *International Journal of Control*, in press.

[16] C. Scherer and C. Ebenbauer, "Convex synthesis of accelerated gradient algorithms," 2021. [Online]. Available: https://arxiv.org/abs/2102.06520

[17] J. M. Borwein and D. Noll, "Second order differentiability of convex functions in banach spaces," *Transactions of the American Mathematical Society*, pp. 43–81, 1994.

[18] J. Zhang, J. Carrasco, and W. Heath, "Duality bounds for discrete-time Zames-Falb multipliers," 2020. [Online]. Available: https://arxiv.org/abs/2008.11975

[19] R. A. Freeman, "Noncausal Zames-Falb multipliers for tighter estimates of exponential convergence rates," in *2018 Annual American Control Conference (ACC)*, June 2018, pp. 2984–2989.